

AN ARBITRARY LAGRANGIAN-EULERIAN BASED FINITE ELEMENT FOR SIMULATING CAPILLARY FLOWS

Felipe Montefusco, Fabrício S. Sousa and Gustavo C. Buscaglia

Group on Computational Micro- and Bio-fluid Dynamics, Universidade de São Paulo, Av. Trabalhador São-carlense, 400, São Carlos, São Paulo, Brazil

Keywords: Finite element, Arbitrary Lagrangian-Eulerian, Capillarity, Crank-Nicolson

Abstract. The numerical simulation of dynamic wetting phenomena at small length scales, where capillary forces must be taken into account, is considered. We introduce an arbitrary Lagrangian-Eulerian (ALE) formulation for two and three-dimensional sliding droplet simulations. The explicit representation of phase-separating interfaces in the mesh allows for accurate treatment of surface tension. Boundary conditions, including conditions for the controversial contact lines, are naturally incorporated by means of the finite element method (FEM). The dependence of the capillary forces on the geometry introduces a strong nonlinearity on the system of equations. A scheme of time discretization where the geometry is decoupled from the other variables is presented. Optimal temporal convergence for velocity and pressure can be obtained by an extrapolated Crank-Nicolson method in ALE moving grids, as shown by preliminary numerical experiments.

1 INTRODUCTION

The numerical simulation of flows with interfaces, specially capillary flows in the presence of the contact lines, has been carried out by many authors using the arbitrary Lagrangian-Eulerian (ALE) framework (Walkley and Gaskell (2005), Gerbeau and Lelièvre (2009), Sprittles and Shikhmurzaev (2012), Rabier and Medale (2003)). One of the main reasons for that is that the ALE framework allows an accurate representation of surface forces like surface tension, membrane effects, etc., compared to front-capturing methods (Popinet and Zaleski, 1999). However, despite the extensive discussion about *geometric conservation laws* (GCLs) and *conservative* and *non-conservative* formulations in ALE literature (see, e.g., Formaggia and Nobile (2004) and references therein), time convergence has been ignored in this scenario. For instance, there is nothing in the literature (to the best of our knowledge) reporting second order time convergence of the Crank-Nicolson method (CN) applied to the capillary equations in ALE formulation (or related equations where the ALE mesh velocity depends on the other variables). In Reusken and Esser (2013), which also is in the capillarity context, it is shown optimal convergence for CN but for a fixed grid based method. The work of Nobile (2001) presents a complete stability analysis for both conservative and non-conservative ALE formulation addressing GCLs. Nevertheless, his non-conservative formulation for convection–diffusion equations did not result in optimal convergence for velocity in our tests for capillary equations. In the studies of Étienne et al. (2009), where the addressed problem does not have interface and the mesh velocity is known, only sub-optimal convergence is obtained for the CN/non-conservative formulation.

In this study we will follow the formulation for capillary flows presented in Buscaglia and Ausas (2011) and discuss its numerical aspects in the ALE framework. The surface tension is accounted for weakly in the variational formulation by the Laplace-Beltrami representation of the curvature. We will present an extrapolated CN where the mesh velocity, which is also an unknown, is decoupled from the other variables \mathbf{u} - p and treated explicitly. The price for this extrapolation simplification is a CFL constraint introduced by capillary waves Brackbill et al. (1992), but this issue will only be addressed in further studies. Our concern relies on the temporal convergence of the velocity \mathbf{u} and pressure p in the presence of geometry-dependent forces. We also present some numerical experiments that show quadratic convergence for the velocity and pressure for capillary equations.

2 THE DYNAMIC WETTING EQUATIONS

As in most of the literature on capillary phenomena, we focus on incompressible flows of Newtonian fluids where surface inertial effects are neglected. The specific case of solid-liquid-gas flow is considered, where constant pressure, zero viscosity and zero mass density are assumed for gas phase. The Navier-Stokes equations for the liquid phase occupying a time dependent region $\Omega(t) \subset \mathbb{R}^d$ reads:

$$\frac{\partial(\rho\mathbf{u})}{\partial t} + \mathbf{u} \cdot \nabla(\rho\mathbf{u}) = -\nabla p + \nabla \cdot (2\mu D\mathbf{u}) + \rho\mathbf{g}, \quad \mathbf{x} \in \Omega(t) \quad (1a)$$

$$\nabla \cdot \mathbf{u} = 0 \quad \mathbf{x} \in \Omega(t) \quad (1b)$$

where \mathbf{u} is the fluid velocity, p the pressure, ρ the mass density, μ the dynamic viscosity, \mathbf{g} a body force (e.g. gravity) and $D = 1/2(\nabla + \nabla^T)$ the symmetric gradient operator. In slip models context, the capillary forces at liquid-gas interface (Γ), liquid-solid interface (Γ_s) as well at contact line ($\partial\Gamma_s$) and the classic Navier-type slip law are modeled as the following boundary

conditions (Buscaglia and Ausas, 2011):

$$\boldsymbol{\sigma} \cdot \mathbf{n} = -\gamma \kappa \mathbf{n} + \nabla_{\Gamma} \gamma, \quad \mathbf{x} \in \Gamma, \quad (2a)$$

$$(\mathbf{I} - \mathbf{nn}) \cdot \boldsymbol{\sigma} \cdot \mathbf{n} = -\beta (\mathbf{I} - \mathbf{nn}) \cdot (\mathbf{u} - \mathbf{u}_s), \quad \mathbf{x} \in \Gamma_s, \quad (2b)$$

$$\mathbf{u} \cdot \mathbf{n} = \mathbf{u}_s \cdot \mathbf{n}, \quad \mathbf{x} \in \Gamma_s, \quad (2c)$$

$$\cos \theta(\mathbf{x}, t) - \cos \theta_s = -\zeta (\mathbf{u} - \mathbf{u}_s) \cdot \boldsymbol{\nu}_s / \gamma, \quad \mathbf{x} \in \partial \Gamma_s, \quad (2d)$$

where \mathbf{I} is the identity tensor, \mathbf{n} the outward normal, θ the dynamic contact angle, $\nabla_{\Gamma} \doteq (\mathbf{I} - \mathbf{nn}) \cdot \nabla$ the surface gradient operator, $\kappa = \nabla_{\Gamma} \cdot \mathbf{n}$ the mean curvature positively counted with respect to the normal, $\boldsymbol{\sigma}$ the Cauchy stress tensor, γ the liquid-gas surface tension, \mathbf{u}_s the solid velocity, θ_s the static contact angle, β the slip coefficient and ζ a parameter of the contact line dissipation force model. The contact angle is defined by the relation

$$\cos \theta = \boldsymbol{\nu} \cdot \boldsymbol{\nu}_s, \quad (3)$$

where $\boldsymbol{\nu}$ and $\boldsymbol{\nu}_s$ are the liquid-gas and solid-liquid surfaces conormals, respectively. The surfaces and the contact lines evolution are also unknowns. Here, we suppose that the bounding surface is the same the material surface at all time, i.e., a particle $\varphi(\cdot, t) : \Omega(0) \rightarrow \Omega(t)$ initially belonging to a surface remains at the surface:

$$\varphi(\mathbf{x}, t = 0) \in \Gamma(t = 0) \Leftrightarrow \varphi(\mathbf{x}, t) \in \Gamma(t). \quad (4)$$

To close the system, a compatible initial velocity field $\mathbf{u}_0(\mathbf{x})$ and an initial configuration $\Gamma(t = 0)$ is given.

3 NUMERICAL APPROACH

3.1 Arbitrary Lagrangian-Eulerian method

The idea of the ALE method is to rewrite the time derivatives at a point \mathbf{x} fixed in space (denoted by ∂_t) at time t in terms of the time derivative along a pathline $\mathcal{A}^{-1}(\mathbf{x}, t)$ (ALE time derivative ∂_t^*) defined by an arbitrary velocity field $\mathbf{v}(\mathbf{x}, t)$, namely

$$\partial_t = \partial_t^* - (\mathbf{v} \cdot \nabla), \quad \mathbf{v}(\mathbf{x}, t) \doteq \frac{\partial \mathcal{A}}{\partial t} \circ \mathcal{A}_t^{-1}(\mathbf{x}, t), \quad (5)$$

where the diffeomorphism \mathcal{A} is constructed according to \mathbf{v} and takes a point from the reference domain $\hat{\Omega} = \Omega(t = 0)$ to the current domain $\Omega(t)$. The advantage of this formulation is that one can move the mesh arbitrarily while the time integration of a quantity can still be made entirely at the mesh's vertices as in Eulerian frames. The ALE formulation of the Navier-Stokes equations (1), where we will assume constant mass density, is given by

$$\rho (\partial_t^* \mathbf{u} + (\mathbf{c} \cdot \nabla) \mathbf{u}) = \nabla \cdot \boldsymbol{\sigma} + \rho \mathbf{g}, \quad \mathbf{x} \in \Omega, \quad (6)$$

$$\nabla \cdot \mathbf{u} = 0, \quad \mathbf{x} \in \Omega, \quad (7)$$

where we defined $\mathbf{c} \doteq \mathbf{u} - \mathbf{v}$ (convective velocity) for the sake of simplicity. Because it is desired that the mapping \mathcal{A} follows the domain's shape, the velocity field must satisfy the condition

$$\mathbf{v} \cdot \mathbf{n} = \mathbf{u} \cdot \mathbf{n} \quad (8)$$

on the entire boundary $\partial \Omega = \Gamma \cup \Gamma_s$ at all times.

3.2 Variational Formulation

In order to present the variational formulation, we define the following Sobolev spaces

$$W_0 \doteq \left\{ \mathbf{w} \in (H^1(\Omega))^d \mid \mathbf{w} \cdot \mathbf{n} = 0 \text{ on } \Gamma_s \right\}, \quad (9a)$$

$$W_u \doteq \left\{ \mathbf{w} \in (H^1(\Omega))^d \mid \mathbf{w} \cdot \mathbf{n} = \mathbf{u}_s \cdot \mathbf{n} \text{ on } \Gamma_s \right\}, \quad (9b)$$

$$Q \doteq L^2(\Omega) \quad (\text{or } L^2(\Omega)/\mathbb{R} \text{ if needed}), \quad (9c)$$

where $H^1(\Omega)$ and $L^2(\Omega)$ are the usual Sobolev spaces. The corresponding variational formulation of the problem is: for all $(\mathbf{w}, q) \in W_0 \times Q$, find $(\mathbf{u}, p) \in W_u \times Q$ such that $\mathbf{u}(\mathbf{x}, t = 0) = \mathbf{u}_0(\mathbf{x})$ and

$$\begin{aligned} & \int_{\Omega} [\rho (\partial_t^* \mathbf{u} + [(\mathbf{c} \cdot \nabla) \mathbf{u}]) \cdot \mathbf{w} + (2\mu D\mathbf{u} - p\mathbf{I}) : D\mathbf{w}] + \\ & + \int_{\Gamma_s} \beta (\mathbf{u} - \mathbf{u}_s) \cdot \mathbf{w} + \int_{\partial\Gamma} \zeta ((\mathbf{u} - \mathbf{u}_s) \cdot \boldsymbol{\nu}_s) (\mathbf{w} \cdot \boldsymbol{\nu}_s) = \int_{\Omega} \rho \mathbf{g} - \int_{\Gamma} \gamma \nabla_{\Gamma} \cdot \mathbf{w} + \end{aligned} \quad (10a)$$

$$\begin{aligned} & + \int_{\partial\Gamma} \gamma \cos \theta_s \mathbf{w} \cdot \boldsymbol{\nu}_s, \\ & \int_{\Omega} q \nabla \cdot \mathbf{u} = 0, \end{aligned} \quad (10b)$$

where $\Omega = \mathcal{A}(\hat{\Omega}, t)$, and also find any smooth mapping such that

$$(\mathbf{u} - \mathbf{v}) \cdot \mathbf{n} = 0, \quad \mathbf{x} \in \partial\Omega. \quad (11)$$

The construction of \mathcal{A} and its restriction (11) will be discussed after discretization, while the derivation of capillarity terms in the variational formulation can be found in [Buscaglia and Ausas \(2011\)](#). Henceforth we simplify our model by supposing a fixed wall ($\mathbf{u}_s = \mathbf{0}$) so that we can consider the trial and tests functions in a same space $W (= W_0 = W_u)$.

3.3 Discretization in space

Let $\mathcal{T}_h(t)$ be a mesh partition of the domain $\Omega(t)$, and W_h and Q_h be the finite element subspaces of W and Q , respectively, whose bases are polynomials in each simplex $K \in \mathcal{T}_h$ and are chosen to be nodal interpolation functions, for simplicity. We distinguish all fields (velocity, pressure, normal, etc.) and sets (Ω , Γ , etc.) from their discrete counterpart by a subscript h . The velocity \mathbf{u}_h and pressure p_h approximations are written by

$$\mathbf{u}_h(\mathbf{x}, t) = \sum_j \phi^j(\mathbf{x}, t) \mathbf{u}^j(t), \quad \phi^j(\cdot, t) \mathbf{e}_{\alpha} \in W_h, \quad (12a)$$

$$p_h(\mathbf{x}, t) = \sum_k \psi^k(\mathbf{x}, t) p^k(t), \quad \psi^k(\cdot, t) \in Q_h, \quad (12b)$$

where \mathbf{e}_{α} , $\alpha = 1, \dots, d$, are \mathbb{R}^d canonical base's vectors and \mathbf{u}^j and p^k are variables coefficients with nodal value meaning. We use *isoparametric* interpolation in order to maintain optimal spatial convergence when a high order polynomial for velocity is used. Thus, the semi-discrete version of the mesh velocity is given by

$$\mathbf{v}_h(\mathbf{x}, t) = \sum_j \phi^j(\mathbf{x}, t) \mathbf{V}^j(t), \quad (13)$$

where the coefficient \mathbf{V}^j is the velocity of the j th node.

We assume that the problem has a unique solution $(\mathbf{u}_h, p_h) \in W_h \times Q_h$ with the following error estimation

$$\|\mathbf{u} - \mathbf{u}_h\|_{W_u} + \|p - p_h\|_{Q_h} \leq C \left(\inf_{\mathbf{w}_h \in W_h} \|\mathbf{u} - \mathbf{w}_h\|_{W_h} + \inf_{q_h \in Q_h} \|p - q_h\|_{Q_h} \right). \quad (14)$$

3.4 Some finite elements

In this study, we use the LBB stable element P_2P_1 (piecewise quadratic polynomial for velocity and piecewise linear for pressure). We also test the stabilized element P_1P_1 (ASGS) presented in Codina (2001) (this stabilization is identical to the *Galerkin-least squares* for linear elements) and the mini-element $P_1^+P_1$. We intend to assess the impact of these stabilization terms in the time convergence of our ALE framework.

3.5 Discretization in time

We use the superscript n to refer to the time level $t^n = n\Delta t$, where the time step $\Delta t \doteq t^{n+1} - t^n$ is chosen to be constant. We also use the notation

$$f^{n+\theta} \doteq \theta f^{n+1} + (1 - \theta)f^n, \quad \delta f^n \doteq f^{n+1} - f^n \quad \text{and} \quad \delta_t^n f \doteq \frac{\delta f^n}{\Delta t}. \quad (15)$$

In this study, we consider a piecewise linear time approximation of the mesh motion. Let $\mathcal{A}_h^n(\mathbf{y})$ be a parametrization of the mesh geometry at the instant t^n given by

$$\mathcal{A}_h^n(\mathbf{y}) = \sum_j \hat{\phi}^j(\mathbf{y}) \mathbf{X}^j(t^n), \quad (16)$$

where \mathbf{X}^j is the coordinate of the j th node and $\hat{\phi}^j = \phi^j(\cdot, t^n) \circ \mathcal{A}_h^n$. In this way, for each time interval $(t^n, t^{n+1}]$, we have

$$\mathcal{A}_h(\mathbf{y}, t) = \mathcal{A}_h^{n+1}(\mathbf{y}) \frac{t - t^n}{\Delta t} + \mathcal{A}_h^n(\mathbf{y}) \frac{t^{n+1} - t}{\Delta t}, \quad t \in (t^n, t^{n+1}]. \quad (17)$$

The time derivative of the previous mapping leads to a constant mesh velocity given by

$$\hat{\mathbf{v}}_h(\mathbf{y}, t) \doteq \frac{\mathcal{A}_h^{n+1}(\mathbf{y}) - \mathcal{A}_h^n(\mathbf{y})}{\Delta t}, \quad t \in (t^n, t^{n+1}]. \quad (18)$$

It means that each node of the mesh moves with a constant velocity in each time interval $(t^n, t^{n+1}]$. This velocity expressed in current frame is given by

$$\mathbf{v}_h(\mathbf{x}, t) = \hat{\mathbf{v}}_h(\mathcal{A}_h^{-1}(\mathbf{x}, t)), \quad t \in (t^n, t^{n+1}], \quad (19)$$

and is discontinuous at times t^n .

We focus here on the extrapolated Crank-Nicolson method. Applying it on the scheme of (10), we have the following problem statement: for a given \mathcal{A}_h^n , an extrapolation of \mathcal{A}_h^{n+1} and

$[\mathbf{u}_h \in W_h]^n$, find $[(\mathbf{u}_h, p_h) \in W_h \times Q_h]^{n+1}$ such that, for all $[(\mathbf{w}_h, q_h) \in W_h \times Q_h]^{n+1/2}$,

$$\begin{aligned} & \int_{\Omega_h^{n+1/2}} \rho \left(\delta_t^n \mathbf{u}_h + \nabla \mathbf{u}_h^{n+1/2} \cdot \mathbf{c}_h^{n+1/2} \right) \cdot \mathbf{w}_h + \\ & + \int_{\Omega_h^{n+1/2}} (-\mathbf{I}_d r^{n+1} + 2\mu D\mathbf{u}_h^{n+1/2}) : D\mathbf{w}_h + \\ & + \int_{\Gamma_{h,s}^{n+1/2}} \beta \mathbf{u}_h^{n+1/2} \cdot \mathbf{w}_h = - \int_{\Gamma_h^{n+1/2}} \gamma \nabla_{\Gamma} \cdot \mathbf{w}_h \\ & + \int_{\partial\Gamma_h^{n+1/2}} \gamma \cos \theta_s \boldsymbol{\nu}_s \cdot \mathbf{w}_h - \int_{\partial\Gamma_h^{n+1/2}} (\zeta \mathbf{u}_h^{n+1/2} \cdot \boldsymbol{\nu}_s) (\mathbf{w}_h \cdot \boldsymbol{\nu}_s); \end{aligned} \quad (20a)$$

$$\int_{\Omega_h^{n+1/2}} \nabla \cdot \mathbf{u}_h^{n+1/2} = 0, \quad (20b)$$

where $\Omega_h^{n+1/2}$ is the domain computed with the average of \mathcal{A}_h^n and (extrapolated) \mathcal{A}_h^{n+1} . The r^{n+1} term is the approximation of the pressure at the mid step, i.e.,

$$\lim_{\Delta t \rightarrow 0} r^{n+1} = p_h(\cdot, t^{n+1/2}). \quad (21)$$

Thus, to find the pressure at time t^n a post-processing is needed.

Remark One could consider to replace r^{n+1} by $p_h^{n+1/2} = (1/2)(p_h^{n+1} + p_h^n)$. However, in this approach an initial pressure $p_h(\cdot, 0)$ must be specified. The problem is that this initial field must satisfy a compatibility condition for the quantities $\|\mathbf{u}_h(\cdot, t)\|_{\mathbf{H}^3}$ and $\|\partial_t \mathbf{u}_h(\cdot, t)\|_{\mathbf{H}^1}$ to be bounded.

When a function defined on a domain $\Omega^{n+\alpha}$ appears in a integral over a different domain $\Omega^{n+\theta}$, where $\alpha, \theta \in [0, 1]$, it means that this function is transported onto $\Omega^{n+\theta}$ by an ALE mapping $\mathcal{A}_h^{n+\alpha, n+\theta}$ given by

$$\mathcal{A}_h^{n+\alpha, n+\theta} \doteq \mathcal{A}_h^{n+\theta} \circ (\mathcal{A}_h^{n+\alpha})^{-1}. \quad (22)$$

For example, the first term in (20) we write

$$\int_{\Omega_h^{n+1/2}} \mathbf{u}_h^{n+1} \cdot \mathbf{w}_h \quad (23)$$

for what should be

$$\int_{\Omega_h^{n+1/2}} (\mathbf{u}_h^{n+1} \circ \mathcal{A}_h^{n+1/2, n+1}) \cdot \mathbf{w}_h \quad (24)$$

Now we present how \mathcal{A}_h^{n+1} is extrapolated to complete the overview of the method.

4 GEOMETRY EXTRAPOLATION

Due the integrations on $\Omega_h^{n+1/2}$ which are computed with $\mathcal{A}_h^{n+1/2}$, the geometry is nonlinearly coupled with other variables \mathbf{u}_h^{n+1} and r^{n+1} by all equations. To eliminate this type of nonlinearity and to reduce the number of unknowns of the system, we perform a second order linearization. At time step n , given \mathbf{u}_h^n , \mathbf{u}_h^{n-1} , and the mesh \mathcal{A}_h^n , we do the following: we

move the coordinates of \mathcal{A}_h^n with the vector field \mathbf{v}_h (the mesh velocity) obtained from a linear elasticity problem of the form

$$\mathcal{L}(\mathbf{v}_h) = \mathbf{0}, \tag{25}$$

where \mathcal{L} is a linear second order operator. As Dirichlet boundary conditions, an extrapolation of the fluid velocity at time $\mathbf{u}_h^{n+1/2}$ is used:

$$\mathbf{v}_h^{n+1/2} = \frac{1}{2}(3\mathbf{u}_h^n - \mathbf{u}_h^{n-1}), \quad \mathbf{x} \in \Gamma. \tag{26}$$

Rewriting (18), we obtain the expression of the extrapolated mesh, given by

$$\mathcal{A}_h^{n+1} = \mathcal{A}_h^n + \hat{\mathbf{v}}_h^{n+1/2} \Delta t. \tag{27}$$

Then, we proceed and solve the system (20). One can use the obtained velocity \mathbf{u}_h^{n+1} to recompute a better \mathbf{v}_h and solve the system (20) again, like a predictor–corrector algorithm. To save computation effort, we do this only in the first time step, where \mathbf{u}_h^{n-1} is not defined as well as the ansatz (26). This idea of using an extrapolated velocity is similar to the one proposed in Gerbeau and Lelièvre (2009). As will be seen in results, this strategy does not affect the second order accuracy of the velocity of the original CN, even in the presence of the capillary terms that depend on the geometry.

5 MESH MOVEMENT SMOOTHING

Ideally, the Eq. (25) must be such that its solution \mathbf{v}_h is a smooth extension of the boundary displacement $\mathbf{v}_h \Delta t$, so that the good quality of the mesh elements is maintained. We have chosen to use a variant of a linear elasticity equation proposed by Dwight (2009). Therein, the Lamé constants λ and μ of the linear elasticity equation

$$\nabla \cdot (\lambda \text{Tr}(D\mathbf{v})\mathbf{I} + 2\mu D\mathbf{v}) = \mathbf{0} \tag{28}$$

are chosen to be $\lambda = -\mu = E$, where E is the Young’s modulus and is element-wise constant (equals to inverse of the element volume). With those choices, the equation admits rigid motions as solution. The author Dwight (2009) emphasizes that the equations can no longer be thought of as a model of elasticity, although they behave somewhat similarly. In his results, he has achieved up to 70% greater mesh rotations in some tests compared to standard linear elasticity model.

6 NUMERICAL RESULTS

In this section, we present some numerical assessment of the ALE formulation. The first two problems are manufactured solutions, where the force term \mathbf{g} and the boundary force (Neumann boundary condition) is such that the Navier-Stokes is satisfied. In these tests, the velocity $\mathbf{v}_h^{n+1/2}$ computed in Eq. (20a) is prescribed by the user, thus the geometry is known and there is no extrapolation. The last problem is the three dimensional capillary equations. In this test, the geometry is extrapolated as described in Sec.(4) and geometry-dependent forces are present.

6.1 Manufactured solution I (MS1)

We consider a kind of Couette flow, with $\rho = \mu = 1$, such that the exact solution is given by

$$\mathbf{u} = (x \cos(t) + y \sin(t), x \sin(t) - y \cos(t)), \tag{29}$$

$$p = x \cos(t) + y \sin(t), \tag{30}$$

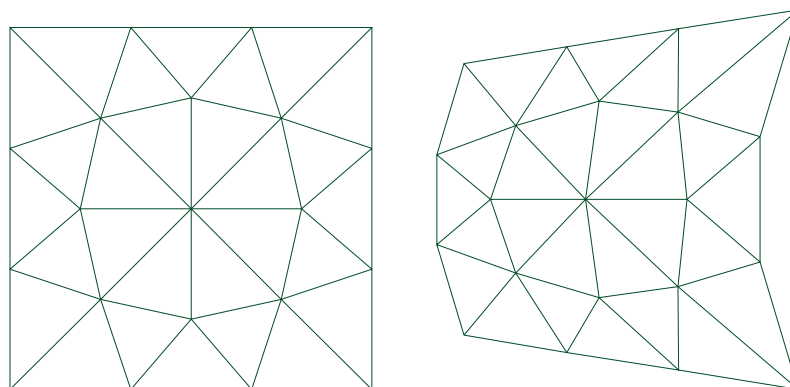


Figure 1: Mesh used for the MS1 and MS2 tests. On the left is the initial mesh and on the right is the mesh at the final state of the simulation.

k	$P_1^+ P_1$			
	e_u	order	e_p	order
3	9.097e-05	–	4.206e-05	–
4	2.275e-05	1.999	1.057e-05	1.991
5	5.688e-06	1.999	2.652e-06	1.995
6	1.422e-06	1.999	6.640e-07	1.997
7	3.555e-07	1.999	1.661e-07	1.999
8	8.889e-08	2.000	4.155e-08	1.999
9	2.222e-08	2.000	1.039e-08	1.999
10	5.556e-09	2.000	2.597e-09	1.999

Table 1: Time convergence of the problem MS1.

where $(x, y) \doteq \mathbf{x}$. Note that \mathbf{u} and p are linear in \mathbf{x} , so the only source of errors is due the time discretization. The mesh velocity is chosen to be

$$\mathbf{v} = (x^2 \sin(t) + y^2 \cos(t), -xy \sin(t) + xy \cos(t)), \quad (31)$$

and the initial mesh is the square $[-1.2, 1.2]^2$ (see Fig. (1)). We have taken the time steps $\Delta t = 0.1 \cdot 2^{-k}$, $k = 3, \dots, 10$, and we have computed the velocity error $e_u = \|\mathbf{u}_h - \mathbf{u}\|_{\mathbf{H}^1}$ and the pressure error $e_p = \|p_h - p\|_{L^2}$ errors at time $T = 0.1$. The choices of T and \mathbf{v} are such that the distortion of the final mesh is comparable to the edge size of the coarsest mesh. As can see in Tables 1 and 2, all the elements $P_1^+ P_1$, $P_1 P_1$ (ASGS) and $P_2 P_1$ present optimal convergence.

6.2 Manufactured solution II (MS2)

To exercise more terms of the Navier-Stokes equations, we consider a more complex non-physical flow given by

$$\mathbf{u} = (x^2 y \sin(t), -x y^2 \sin(t)), \quad (32)$$

$$p = x^2 \cos(t) + y^2 \sin(t). \quad (33)$$

Here, we take smaller time steps than previously in order to reach the asymptotic behavior: $\Delta t = 0.001 \cdot 2^{-k}$, $k = 3, \dots, 7$. The mesh is moved by the same velocity of Eq. (31), but it is

k	$P_1P_1(\text{ASGS})$				P_2P_1			
	e_u	order	e_p	order	e_u	order	e_p	order
3	7.116e-05	–	4.425e-05	–	6.442e-05	–	3.292e-05	–
4	1.782e-05	1.997	1.112e-05	1.991	1.611e-05	1.999	8.230e-06	2.000
5	4.460e-06	1.998	2.788e-06	1.996	4.027e-06	1.999	2.057e-06	2.000
6	1.115e-06	1.999	6.981e-07	1.998	1.007e-06	1.999	5.144e-07	2.000
7	2.789e-07	1.999	1.746e-07	1.999	2.517e-07	2.000	1.286e-07	2.000
8	6.974e-08	1.999	4.368e-08	1.999	6.294e-08	2.000	3.215e-08	2.000
9	1.743e-08	1.999	1.092e-08	1.999	1.573e-08	2.000	8.037e-09	2.000
10	4.359e-09	2.000	2.730e-09	1.999	3.934e-09	2.000	2.009e-09	2.000

Table 2: Time convergence of the problem MS1.

k	$P_1P_1(\text{ASGS})$				P_2P_1			
	e_u	order	e_p	order	e_u	order	e_p	order
3	2.682e-07	–	1.077e-04	–	2.478e-07	–	1.211e-04	–
4	6.702e-08	2.001	2.693e-05	2.000	6.194e-08	2.000	3.027e-05	2.000
5	1.674e-08	2.000	6.733e-06	2.000	1.548e-08	2.000	7.569e-06	2.000
6	4.184e-09	2.001	1.683e-06	2.000	3.870e-09	2.000	1.892e-06	2.000
7	1.044e-09	2.002	4.205e-07	2.000	9.674e-10	2.000	4.729e-07	2.000
8	2.603e-10	2.004	1.049e-07	2.002	2.416e-10	2.001	1.181e-07	2.001

Table 3: Time convergence of the problem MS2.

multiplied by a factor of 50 to compensate the small time step. Unlike what happens in MS1, the solution (32)–(33) is not represented exactly by any spatial discretization. In order to compute only the temporal error, we subtract the solution from a reference solution \mathbf{u}_{ref} computed by the Richardson extrapolation of the obtained solutions sequence. Thus, we redefine the errors to

$$e_u = \|\mathbf{u}_h(\cdot, T) - \mathbf{u}_{ref}(\cdot, T)\|_\infty, \quad e_p = \|p_h(\cdot, T) - p_{ref}(\cdot, T)\|_\infty. \quad (34)$$

Table 3 shows the convergence for $P_1P_1(\text{ASGS})$ and P_2P_1 . We can observe that both elements still with second order convergence for both velocity and pressure, besides the theoretical studies of Heywood and Rannacher (1990) that predicted only first order of converge for pressure.

6.3 Spreading droplet

Herein, a spreading droplet in a total wetting regime is considered. In this test all capillary terms in Eq. (20a) are present: surface tension, surface dissipation, elastic contact line force and concentrated contact line dissipation. Clearly, all of them depends on the geometry. The purpose is to check whether the extrapolation of the mesh velocity affects the convergence of the full Crank-Nicolson. The chosen parameters are: $\rho = 1$, $\mu = 0.1$, $\gamma = 0.01$, $\beta = \zeta = 0.001$, $\mathbf{g} = (0, -1, 0)$ and $\theta_s = 0$ (total wetting). The drop is initially a hemisphere of radius one. Taking advantage of the problem symmetry, only 1/4 of the drop is discretized by the mesh. As in previous test, we extrapolate a reference solution to computed the convergence. We have taken the time steps $\Delta t = 0.01 \cdot 2^{-k}$, $k = 1, 2, 3, 4, 5, 6$ and the errors have computed at $T = 0.3$.

k	e_u	order	e_p	order	e_{vol}	order
1	1.041e-04	–	6.063e-05	–	2.776e-06	–
2	3.505e-05	1.570	1.834e-05	1.724	6.887e-07	2.011
3	1.089e-05	1.687	5.283e-06	1.795	1.714e-07	2.006
4	3.122e-06	1.803	1.451e-06	1.864	4.278e-08	2.003
5	8.444e-07	1.886	3.879e-07	1.903	1.068e-08	2.001
6	2.205e-07	1.937	1.010e-07	1.941	2.669e-09	2.000

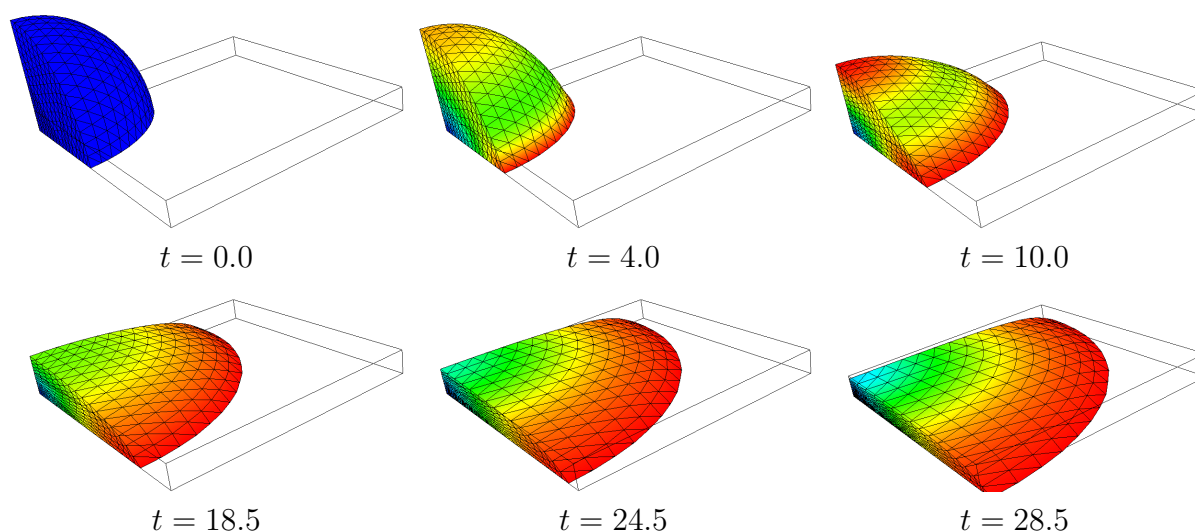
Table 4: Three dimensional droplet time convergence using the element P_2P_1 .

Figure 2: Some frames of the simulation of the spreading droplet in a total wetting regime, where the color scale represents the velocity magnitude (blue corresponds to zero).

Table 4 shows the temporal convergence of the simulation using the P_2P_1 element. We also have included the relative volume error e_{vol} in this table, computed as

$$e_{vol} = \frac{|\text{Volume}_{final} - \text{Volume}_{initial}|}{\text{Volume}_{initial}}. \quad (35)$$

One can note that quadratic convergence is maintained for velocity, pressure and volume despite the extrapolation and all geometry-dependent forces. An illustration of the simulated droplet can be found in Fig. (2).

7 CONCLUSION

We have presented an ALE-FEM formulation to solve capillary equations. We show that second order temporal convergence can be obtained by the ALE formulation in non-conservative form using an extrapolated Crank-Nicolson method. Details of the implementation, often missing or dispersed in the literature, have been presented here. We have validated our code by simple benchmarks and the obtained results shows the applicability of the presented formulation.

ACKNOWLEDGMENTS

The authors gratefully acknowledge the financial support received from FAPESP and CNPq.

REFERENCES

- Brackbill J., Kothe D., and Zemach C. A continuum method for modeling surface tension. *Journal of computational physics*, 100(335-354), 1992.
- Buscaglia G.C. and Ausas R.F. Variational formulations for surface tension, capillarity and wetting. *Computer Methods in Applied Mechanics and Engineering*, 200(45-46):3011–3025, 2011. ISSN 00457825. doi:10.1016/j.cma.2011.06.002.
- Codina R. A stabilized finite element method for generalized stationary incompressible flows. *Computer Methods in Applied Mechanics and*, 190:2681–2706, 2001.
- Dwight R. Robust mesh deformation using the linear elasticity equations. *Computational Fluid Dynamics 2006*, 2009.
- Étienne S., Garon a., and Pelletier D. Perspective on the geometric conservation law and finite element methods for ALE simulations of incompressible flow. *Journal of Computational Physics*, 228(7):2313–2333, 2009. ISSN 00219991. doi:10.1016/j.jcp.2008.11.032.
- Formaggia L. and Nobile F. Stability analysis of second-order time accurate schemes for ALE–FEM. *Computer Methods in Applied Mechanics and Engineering*, 193(39-41):4097–4116, 2004. ISSN 00457825. doi:10.1016/j.cma.2003.09.028.
- Gerbeau J.F. and Lelièvre T. Generalized Navier boundary condition and geometric conservation law for surface tension. *Computer Methods in Applied Mechanics and Engineering*, 198(5-8):644–656, 2009. ISSN 00457825. doi:10.1016/j.cma.2008.09.011.
- Heywood J. and Rannacher R. Finite-element approximation of the nonstationary Navier-Stokes problem. Part IV: Error analysis for second-order time discretization. *SIAM Journal on Numerical Analysis*, 27(2):353–384, 1990.
- Nobile F. Numerical approximation of fluid-structure interaction problems with application to haemodynamics. *PhD, Ecole Polytechnique Fédérale de Lausanne, Switzerland*, 2001.
- Popinet S. and Zaleski S. A front-tracking algorithm for accurate representation of surface tension. *International Journal for Numerical Methods in Fluids*, 30(6):775–793, 1999. ISSN 02712091. doi:10.1002/(SICI)1097-0363(19990730)30:6<775::AID-FLD864>3.3.CO;2-R.
- Rabier S. and Medale M. Computation of free surface flows with a projection FEM in a moving mesh framework. *Computer Methods in Applied Mechanics and Engineering*, 192(41-42):4703–4721, 2003. ISSN 00457825. doi:10.1016/S0045-7825(03)00456-0.
- Reusken A. and Esser P. Analysis of time discretization methods for Stokes equations with a nonsmooth forcing term. *Numerische Mathematik*, pages 1–27, 2013. ISSN 0029-599X. doi:10.1007/s00211-013-0564-2.
- Sprittles J.E. and Shikhmurzaev Y.D. Finite Element Framework for Describing Dynamic Wetting Phenomena. *International Journal for Numerical Methods in Fluid*, 68(10):1257–1298, 2012. doi:10.1002/fld.
- Walkley M. and Gaskell P. Finite element simulation of three-dimensional free-surface flow problems with dynamic contact lines. *International Journal for Numerical Methods in Fluids*, 47(December 2004):1353–1359, 2005.